
Temporal2Seq: A Unified Framework for Temporal Video Understanding Tasks

Min Yang

State Key Laboratory for
Novel Software Technology
Nanjing University
yangminmcg1011@hotmail.com

Zichen Zhang

State Key Laboratory for
Novel Software Technology
Nanjing University
zichenzhang@smail.nju.edu.cn

Limin Wang

State Key Laboratory for
Novel Software Technology
Nanjing University
lmwang@nju.edu.cn

Abstract

With the development of video understanding, there is a proliferation of tasks for clip-level temporal video analysis, including temporal action detection (TAD), temporal action segmentation (TAS), and generic event boundary detection (GEBD). While task-specific video understanding models have exhibited outstanding performance in each task, there remains a dearth of a unified framework capable of simultaneously addressing multiple tasks, which is a promising direction for the next generation of AI. To this end, in this paper, we propose a single unified framework, coined as **Temporal2Seq**, to formulate the output of these temporal video understanding tasks as a sequence of discrete tokens. With this unified token representation, Temporal2Seq can train a generalist model within a single architecture on different video understanding tasks. In the absence of multi-task learning (MTL) benchmarks, we compile a comprehensive co-training dataset by borrowing the datasets from TAD, TAS, and GEBD tasks. We evaluate our Temporal2Seq generalist model on the corresponding test sets of three tasks, demonstrating that Temporal2Seq can produce reasonable results on various tasks and achieve advantages compared with single-task training on this framework. We also investigate the generalization performance of our generalist model on new datasets from different tasks, which yields superior performance to the specific model.

1 Introduction

In recent years, the video understanding community has witnessed a proliferation of video understanding tasks and their associated datasets in different scenarios such as temporal action detection (TAD) [14; 31], temporal action segmentation (TAS) [18; 11; 45], and Generic Event Boundary Detection (GEBD) [43]. Meanwhile, many task-specific models [59; 28; 48; 49; 58; 42; 30] have achieved astonishing results in their tasks. With the rise of large language models (LLMs) [16; 35; 36; 2], a wide range of diverse language-related tasks are unified into a single modeling framework, resulting in remarkable achievements in sequence causal reasoning. Inspired by this, the temporal video understanding community critically demands the unification of multiple tasks with the rapid growth of temporal video data [12; 7]. However, these task-specific models [59; 28; 48] above cannot handle different temporal understanding tasks. Given that few have attempted to unify these temporal video

understanding tasks, how to design a unified architecture in these tasks and take advantage of datasets from different tasks to build a generalist model is a challenge that needs to be solved.

Multi-Task Learning (MTL) [3; 4; 10; 54; 22] has consistently been one of the most popular techniques to solve such challenges. It aims to utilize a single model to train on multiple tasks, jointly improving all tasks across various fields. For example, large language models [2; 16] have successfully trained a single unified model to handle all downstream tasks via an autoregressive architecture. Meanwhile, very few works try to build a unified modeling framework for vision tasks, such as Pixel2Seq V2 [4] or Unified IO [33]. However, these works all focus on image understanding tasks and there has been no attempt to design a unified model to handle different temporal video understanding tasks. Although a few works have realized the importance of establishing a multi-task benchmark [8; 12] in video understanding, there is still a lack of relevant joint training framework. The above situations prohibit the development of generalist model in the video domain. Based on the success of unified modeling in the language and image domain, we aim to extend this promising paradigm to the video domain with a focus on handling temporal understanding tasks.

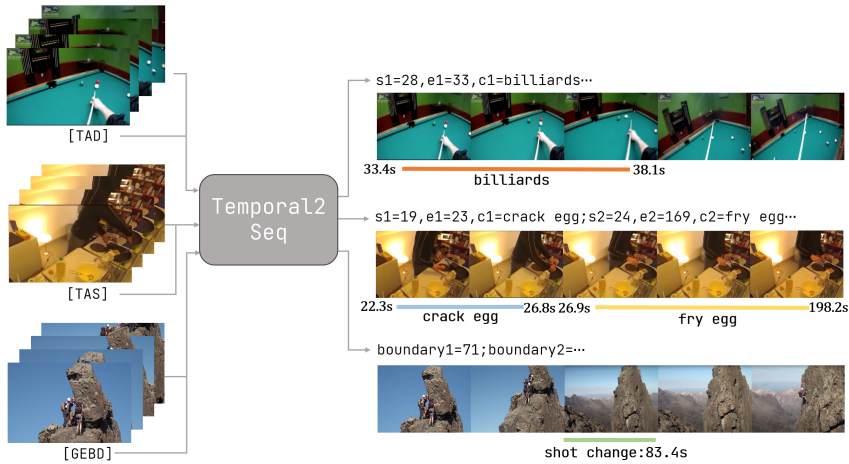


Figure 1: **The overview of Temporal2Seq.** We input video sequences from different tasks and their corresponding task prompts [*TASK*] into the model, the model produces task output tokens which can be detokenized into the required task output for visualization.

To this end, in this paper, we build a single unified framework, termed as **Temporal2Seq**, for different kinds of temporal video understanding tasks with a sequence-to-sequence architecture. As a proof of concept, we choose three tasks, including temporal action detection (TAD), temporal action segmentation (TAS), and generic event boundary detection (GEBD). Inspired by the Pix2Seq V2 [4], our Temporal2Seq framework formulates the output of these three video understanding tasks as a sequence of discrete tokens, as shown in Figure 1. This unified token representation endows our Temporal2Seq with a simple and general interface to handle three tasks within a single framework jointly. To benchmark the performance of Temporal2Seq, we compile a comprehensive benchmark of temporal action understanding tasks by borrowing the datasets from each task and co-train our Temporal2Seq model on these datasets. After training, our single generalist model can perform different video understanding tasks via a simple prompt. The experiment results demonstrate that our single Temporal2Seq model outperforms the baseline counterparts for three tasks. To further investigate the advantage of our Temporal2Seq generalist model, we transfer this unified model to new datasets from different tasks to test its generalization ability, which yields superior performance to the specific model. In summary, our contributions are as follows:

- We propose a single, unified framework for handling temporal video understanding tasks. To our knowledge, our Temporal2Seq is the first unified video modeling framework for handling different types of temporal video understanding tasks without text modality.
- We successfully co-train our Temporal2Seq model on three diverse video understanding tasks, covering detection, segmentation, and timestamp localization. Temporal2Seq could be flexibly applied to different tasks via a simple task prompt.

- Our Temporal2Seq empirically demonstrates the improvement of co-training across all three tasks over each specific model. Our generalist model also achieves competitive performance to established task-specific models under fair conditions. We also show its promising generalization ability on new datasets from these tasks.

2 Related Work

Temporal Action Detection. Temporal action detection (TAD) aims to localize the temporal interval of each action instance in an untrimmed video and recognize its action category.

Due to limited GPU memory, most existing methods [59; 42; 30; 47; 26; 27; 46; 55; 60] use pre-extracted action recognition features as inputs to the TAD model while others trying to train an end-to-end model [56; 25; 29; 5; 52]. Considering the decoding manner, TAD can be divided into actionness-based, anchor-based and query-based methods. Actionness-based [27; 26; 46] adopt a “bottom-up” fashion to generate proposals by locating temporal boundaries and combining them into proposals. Anchor-based [59; 25] regress proposals by fine-tuning anchors [5; 52] or directly generating anchor boundaries. Query-based [47; 30; 42] take a set of proposal queries as input and refine the corresponding query embedding into predictions. Our Temporal2Seq tries a different way that convert action boundaries and class labels into sequences of discrete tokens to generate action predictions.

Temporal Action Segmentation. Temporal Action Segmentation (TAS) aims to classify actions in untrimmed videos and provide frame-by-frame action label predictions. Some early work [39; 15] migrated methods from TAD to TAS tasks through sliding windows and non-maximum suppression. Other work uses Markov model [19; 50] or RNN [9; 57] to model the temporal sequence and then classify framewise actions. With the rise of Temporal Convolutional Networks [20] and Transformer [51], numerous outstanding works have emerged [23; 24; 58; 1; 28], achieving significant success. Our Temporal2Seq adopts a dense prediction paradigm to output the action category of each frame in the form of discrete tokens. These frame-level predictions are then transformed into segment-level action segmentations without any post-processing algorithms.

Generic Event Boundary Detection. Generic event boundary detection (GEBD) aims at locating the general boundaries that divide videos into semantically coherent and taxonomy-free units and could serve as an important pre-processing step for clip-level video understanding. Previous GEBD methods [44; 20; 27; 26; 49] focused on building representations specifically designed for event-level boundaries and exploited a dense prediction paradigm with postprocessing. In contrast to these dense prediction methods, Temporal Perceiver [48] tried a sparse prediction paradigm by constructing boundary queries that directly regress the location of event boundaries. Our Temporal2Seq follows the dense prediction paradigm by predicting whether the current frame is an event boundary.

Multi-Task Learning. The goal of Multi-task learning (MTL) is to train a single model to learn multiple tasks simultaneously. Such approaches offer several advantages including improved data efficiency, reduced overfitting through shared representations, and fast learning by leveraging auxiliary information. The existing methods of MTL [40; 6; 61; 22; 33; 38; 4; 37] have been partitioned into two groups: hard parameter sharing and soft parameter sharing. Hard parameter sharing [3; 37] allows all tasks to share the entire network parameters, except the decision head. Soft parameter sharing [4; 10; 54] allows each task to have its own model. Currently, there is no multi-task learning pipeline focusing on temporal video understanding tasks. We follow Pix2Seq V2 [4] to build a multi-task autoregressive pipeline on three important video understanding tasks, using one modal to solve them all.

3 Method

3.1 Overview

The overall pipeline of Temporal2Seq is depicted in Figure 2, it unifies these three different temporal video understanding tasks into a sequence-to-sequence framework. Given video clips V sampled to the same length for joint training from untrimmed videos of three tasks and annotations A are

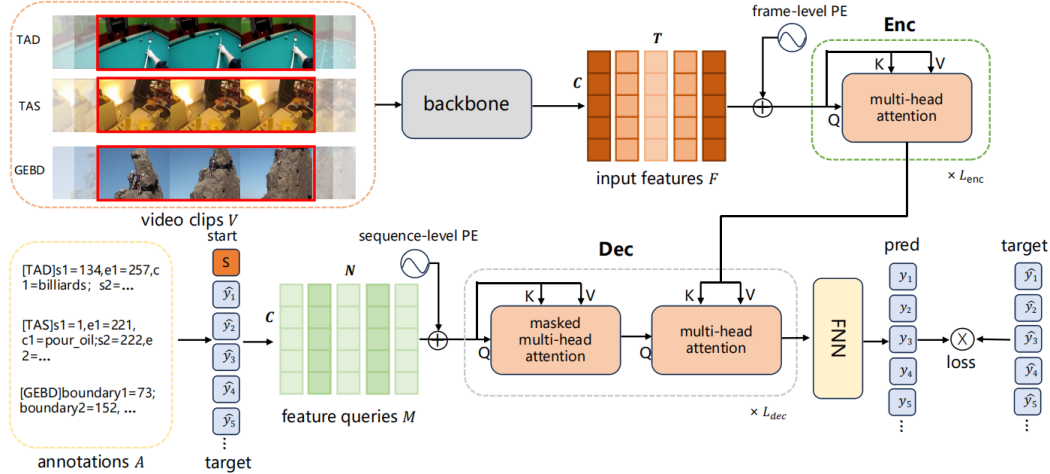


Figure 2: **The overall pipeline of Temporal2Seq.** The input to our model is video features with temporal dimension T extracted by the backbone and a sequence of discrete tokens with token numbers of N translated from annotations. Added with frame-level positional encoding, the encoder maps them into hidden representations. At training time, the decoder takes feature queries M transformed from task annotations A as input and predict the output conditioned by prompt start token, and a loss function is applied afterward. During inference, the decoder generates one token at a time conditioned on the preceding tokens and this process of token generation is repeated until the model provides all predictions. Due to space limitations, H and O are not shown here.

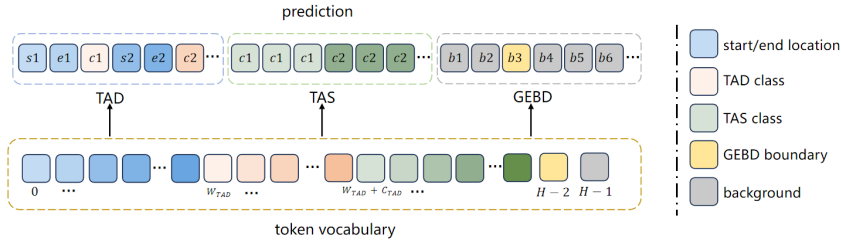


Figure 3: **Construction of token vocabulary.** In the vocabulary, we allocate location tokens for action boundaries and category tokens for all three tasks. During inference, the model generates output tokens one by one, each corresponds to a position in vocabulary.

transformed from the ground truth that action boundaries are normalized to time token space, followed by action categories.

We encode V into frame-level features from backbone [53] and transform them into a latent feature space of reduced dimension $F \in R^{T \times C}$ as input features, where T is the number of frames and C is the feature dimension. Similar to Transformer [51], we add frame-level positional encoding to represent its temporal order. Then the Encoder Enc consisting of L_{enc} layers transforms the input features into hidden representations $H \in R^{T \times C}$ for Decoder Dec consisting of L_{dec} layers.

As to annotations A , We introduce time tokens representing relative timestamps or boundaries and class tokens representing action categories. We formulate them into the target token sequence and add a start token s ($[TAD]$, $[TAS]$ and $[GEBD]$) to the sequence and embed these discrete tokens into query embeddings $M \in R^{N \times C}$ via a dictionary look-up, where N represents the number of target tokens. We add sequence-level positional encoding to represent the order of sequence and then send them into Dec to generate output embeddings $O \in R^{N \times C}$.

After that, a feed-forward network (FFN) maps O back to predicted tokens. The model is trained to maximize the likelihood of token prediction conditioned on previous target tokens with a cross-entropy loss.

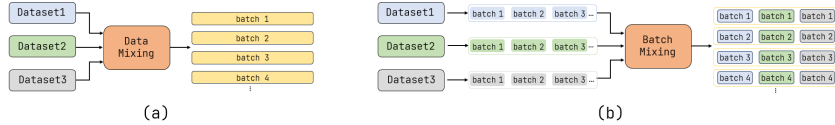


Figure 4: **Mixing ways of training datasets.** (a) Data mixing involves the creation of a dataset that contains mixed frame-target sequence pairs drawn from different tasks and then split into batches for each iteration. (b) Batch mixing samples batches of data from all tasks and then trains the combined batches in each iteration.

3.2 Unified Interface with Tokenization

While TAD, TAS, and GEBD are tasks related to video understanding, these tasks are diverse and traditionally formulated quite differently. TAD needs to localize the start and end of each action and classify their categories. TAS requires the model to generate a dense frame-wise mask for each identified action instance. GEBD has to localize generic event boundaries rather than segment-level prediction. To solve these tasks using a single model, we should provide a unified interface to the task inputs and outputs.

We design such vocabulary with the length of H and employ a consistent color system to represent the type of token shown in Figure 3. We put time tokens representing TAD’s action boundaries, TAD’s action categories, TAS’s action categories, GEBD boundary and background into the token vocabulary. Assuming that we normalize time tokens into $[0, W_{TAD})$, which means that the action boundary has W_{TAD} values. Next, the token vocabulary stores the action categories of TAD and TAS. The token value range of these categories is $[W_{TAD}, W_{TAD} + C_{TAD} + C_{TAS})$ where $C_{[TASK]}$ represents the total number of categories in one task. We place the GEBD boundary and background classes in the last two positions of the token vocabulary for simplicity in code. The length of H should be greater than or equal to the number of tokens required to be encoded.

Specifically, a prediction for TAD can be represented as (s_i, e_i, c_i) which represents the start boundary s , the end boundary e and action’s category c for the i^{th} action, we give consecutive triples like above as predictions. For TAS, we follow previous works [58; 49] and build a dense prediction paradigm without post-processing algorithms. Formally, we classify action categories frame by frame and get predictions $\{c_i\}_{i=1}^L$ where L represents the length of the video frames, and then stitch these per-frame predictions into segment-level action segmentation predictions. For GEBD, it turns into a per-frame binary classification problem, determining whether it is an action boundary or a background frame by frame and getting predictions as $\{b_i\}_{i=1}^L$ where b_i represents whether there is a boundary located at i^{th} temporal location. Then we convert it into a boundary prediction result $\{boundary_i\}_{i=1}^N$ where N is the number of detected boundaries.

During training, the whole vocabulary is used for all three tasks. However, when obtaining predictions for each task during inference, we limit the prediction vocabulary for each task so that each task can only give results within its vocabulary range, avoiding illegal predictions from other tasks appearing in the prediction results of the current task.

3.3 Training

In this section, we will discuss how to train Temporal2Seq on three tasks jointly. We first describe our training strategies, and then introduce our loss function design for each task, especially a new loss function for TAD.

3.3.1 Two Ways of Joint Training

Inspired by Pix2Seq V2 [4], we adopt the following two ways for co-training on different tasks and datasets shown in Figure 4.

In data mixing settings, the datasets of all tasks will be mixed together and divided into multiple groups according to batch size. All these batches will be trained only once within an epoch. We use **Temporal2Seq**_{batch} to represent the model trained in this way.

In batch mixing settings, we pre-partition the dataset into groups based on batch size configuration for each task. After that, a fixed number of batches are randomly selected from these groups and then spliced together for training. It is worth noting that datasets with fewer groups will be input cyclically within the epoch until the datasets with more groups finished their training process. We use **Temporal2Seq_{data}** to represent the model trained in this way.

3.3.2 Data Balance Strategy During Training

In the training process, we observe discrepancies stemming from imbalanced dataset scales and substantial variations in the difficulty levels associated with training tasks across different datasets.

Specifically, the task difficulty of GEBD is lower than that of TAS and TAD, and its excessive data can easily disrupt the training of the other two. To solve such a problem, we propose the data balance strategy by discarding part of the data from the GEBD dataset in advance. By balancing datasets from different tasks, joint training can learn a more general visual representation without being biased towards a certain task. See Appendix A for more details.

3.3.3 Loss Functions

In the original Pix2Seq V2 [4], the unified task was transformed into a standard token classification task. However, this approach can be brutal for TAD, as any prediction that does not regress to the correct location is penalized equally. To relieve this issue, we impose more penalties on predictions further from the ground truth boundaries by building a simple loss function called **weight loss** for TAD based on cross-entropy loss. We adopt cross-entropy loss for both TAS and GEBD. To prevent over-segmentation, we further adopt smooth loss which is widely used in TAS methods [58].

For GEBD, we use the classification loss L_{gebd} as:

$$L_{gebd} = \frac{1}{T} \sum_t -\log(y_{t,\hat{c}}), \quad (1)$$

where T represents the number of input frames, $y_{t,\hat{c}}$ is the predicted probability for the ground truth label \hat{c} at frame t .

For TAS, the loss function L_{tas} is a combination of classification loss L_{cls} for each frame and smooth loss L_{smo} [23] which calculates the mean squared error over the frame-wise probabilities:

$$\begin{aligned} L_{tas} &= L_{cls} + \lambda L_{smo} \\ &= \frac{1}{T} \sum_t -\log(y_{t,\hat{c}}) + \lambda \frac{1}{TC} \sum_t \sum_c (y_{t-1,c} - y_{t,c})^2, \end{aligned} \quad (2)$$

where $y_{t,c}$ is the predicted probability for label c at frame t and C is the total number of action categories. λ represents the weight for L_{smo} .

When predicting boundaries for TAD, we give more penalty to boundary predictions that are further from the ground truth. When predicting action categories, cross-entropy loss is still used. Specifically, we formulate the weight loss and L_{tad} as:

$$L_{weight}(t) = \begin{cases} -\log(y_{t,\hat{c}}) & t \equiv 0 \pmod{3} \\ -(1 + \frac{|\text{argmax}(y_{t,\hat{c}}) - \hat{c}|}{D}) \log(y_{t,\hat{c}}) & t \not\equiv 0 \pmod{3} \end{cases} \quad (3)$$

$$L_{tad} = \frac{1}{T} \sum_t L_{weight}(t), \quad (4)$$

Different from TAS and GEBD, here t represents the current position of outputs instead of frames.

When output action category prediction, L_{weight} is same to cross-entropy loss. When output action's boundary prediction, we need to impose a corresponding penalty based on the distance between the predicted position and the ground truth. Here we use $\text{argmax}(y_{t,\hat{c}})$ to calculate the predicted boundary while the ground truth is \hat{c} . D represents the length of boundary space. Finally, we calculate the prediction loss of the entire sequence, denoted as L_{tad} . For related research, see Appendix C.

With these loss functions, we co-train our Temporal2Seq models **Temporal2Seq_{batch}** in batch-mixing setting and **Temporal2Seq_{data}** in data-mixing setting. We also use the above loss to train the individual model **Baseline_[TASK]** corresponding to each task.

3.4 Inference

During inference, our Temporal2Seq takes the video frames and the corresponding task prompt as input. Our Temporal2Seq starts from the corresponding task prompt token and generates predictions in a sequence format from the model likelihood, i.e., $P(y_j|F, y_{1:j-1})$. For TAD, Temporal2Seq outputs detection predictions as a list of triplets. The confidence of each action is indicated by the classification scores for action categories. We need non-maximum suppression to remove redundant action predictions. For TAS, Temporal2Seq outputs each frame’s action category and combines them into segments. For GEBD, Temporal2Seq outputs each frame’s binary predictions of generic boundaries, and then convert them into locations of boundaries. See Section 3.2 for the specifics of tokenization and Appendix B for more details.

4 Experiments

4.1 Datasets and Evaluation Metrics

We select THUMOS14 and FineAction as our choices for TAD. **THUMOS14** [14] is a classic dataset for TAD task, which contains 413 videos of 30 fps, containing 200 validation videos, and 213 test videos with labeled temporal annotations from 20 categories. **FineAction** [31] is a newly collected large-scale fine-grained TAD dataset containing 57,752 training instances from 8,440 videos and 24,236 validation instances from 4,174 videos and 21,336 testing instances from 4,118 videos. For evaluation, we report the mean average precision (mAP) at different temporal intersections over union (IoU) thresholds [0.3:0.1:0.7] for THUMOS14 and [0.5:0.05:0.95] for FineAction. Avg is the average mAP on these thresholds.

We adopt two widely used TAS datasets [18; 11]. **Breakfast** [18] is the largest and the most challenging dataset among TAS datasets with 1712 videos of 15 fps. A side-view camera records the videos in 18 different kitchens with 48 different actions. **GTEA** [11] contains 28 videos of 11 action classes of daily activities in a kitchen. We use frame-wise accuracy (Acc), segmental edit score (Edit), and segmental overlap F1 score with threshold $k/100$, denoted as $F1@k$, to evaluate the performance. In order to align with other tasks, we do **NOT** perform 5-fold cross-validation adopted by other TAS works [58; 23; 28], and only report results from the first split.

For GEBD, **Kinetics-GEBD** [43] is a recently proposed benchmark, which is derived from Kinetics-400 [17] dataset. It contains 60K YouTube videos with 30 fps that depict various human actions. **TAPOS** [41] contains Olympics sports videos with 21 actions. There are 13,094 training action instances and 1,790 validation action instances. We use the F1 score under different Relative Distance thresholds [0.05 : 0.05 : 0.5] for quality measurement. Avg is the average F1 scores on these thresholds. Due to space limitation, we only report F1 score with a threshold of 0.05 and their average F1 score in the main text. See Appendix F and Appendix G for complete results about all thresholds in related experiments.

We adopt **THUMOS14**, **Breakfast**, and **Kinetics-GEBD** to co-train our Temporal2Seq because they are the most representative in each task, and other datasets will appear in our ablation studies.

4.2 Implementation Details

For all datasets from each task, we adopt ViT-B from [53] for feature extraction and the sampling stride $\tau = 4$ for THUMOS14 and Breakfast, $\tau = 1$ for Kinetics-GEBD. We randomly crop clips of the same length to each video in all three datasets. If the clip lengths are inconsistent, they cannot be divided into batches and trained in parallel. Sliding windows are used during inference to generate predictions. In all experiments, we train the model for 3600 epochs with each epoch involving a randomly sampled clip from each video.

The boundary space D is 150, combined with the fps and sampling stride τ of the respective datasets, we crop each video clip with temporal windows of 20 seconds, 40 seconds, and 5 seconds for THUMOS14, Breakfast, and Kinetics-GEBD. During separate training of individual task model **Baseline**_[TASK], we set batch size 4 for THUMOS14, 32 for Breakfast, and 32 for Kinetics-GEBD. When training them jointly, we set 4 batches for THUMOS14, 28 batches for Breakfast, 32 batches for Kinetics-GEBD for batch-mixing manner called **Temporal2Seq**_{batch}. In data-mixing settings, **Temporal2Seq**_{data} uses a batch size of 32. We use AdamW [32] as optimizer and a learning rate of 2e-

Table 1: **Comparison with baseline models.** We produce baselines for each task to compare with our Temporal2Seq based on data mixing and batch mixing. We report mAP for THUMOS14, F1@{10,25,50}, Edit and Acc for Breakfast, F1 score with a threshold of 0.05 and their average F1 score for Kinetics-GEBD.

Model	Param	TAD						TAS				GEBD		
		0.3	0.4	0.5	0.6	0.7	Avg	F1@{10,25,50}		Edit	Acc	0.05	Avg	
Baseline _{TAD}	11.9M	71.4	64.8	54.9	45.3	30.0	52.9	-	-	-	-	-	-	-
Baseline _{TAS}	11.9M	-	-	-	-	-	-	64.6	60.2	49.2	62.1	61.2	-	-
Baseline _{GEBD}	11.9M	-	-	-	-	-	-	-	-	-	-	-	71.8	84.9
Temporal2Seq _{batch}	11.9M	72.2	65.5	55.6	44.1	30.4	53.6	67.7	61.3	49.4	66.0	61.3	73.3	85.2
Temporal2Seq _{data}	11.9M	71.7	64.8	55.5	44.0	31.2	53.5	66.2	60.8	50.1	64.6	62.3	73.3	85.6

Table 2: **Study on data balance strategy for joint training.** Here we compare the results before and after data sampling of the GEGB dataset. Data sampling has a highly positive effect on the results of the other two tasks.

Model	Data Balance Strategy	TAD						TAS				GEGB		
		0.3	0.4	0.5	0.6	0.7	Avg	F1@{10,25,50}		Edit	Acc	0.05	Avg	
Temporal2Seq _{batch}	✓	72.2	65.5	55.6	44.1	30.4	53.6	67.7	61.3	49.4	66.0	61.3	73.3	85.2
		69.6	60.4	49.5	37.9	26.1	48.3	57.2	53.4	38.5	52.9	54.7	73.3	85.0
Temporal2Seq _{data}	✓	71.7	64.8	55.5	44.0	31.2	53.5	66.2	60.8	50.1	64.6	62.3	73.3	85.6
		70.7	62.7	52.4	40.7	26.9	50.7	55.0	51.6	36.6	51.7	55.1	73.3	85.4

4 following settings from TP [48]. The weight λ is set to 0.15 in Equation 2. $L_{enc} = L_{dec} = 6$. Video frames $L = 150$. We train and test our model based on a single 3090 GPU, since its consumption is less than 8G, worse GPUs are also acceptable.

4.3 Ablation Study

4.3.1 Effectiveness of Co-training on Multiple Tasks

In this section, we present the co-trained results of Temporal2Seq based on two ways and obtain **Temporal2Seq_{data}** and **Temporal2Seq_{batch}**.

As shown in Table 1, all tasks achieve improved performance without introducing additional training parameters compared with **Baseline_{TASK}** for each task. This suggests the existence of semantic sharing between datasets from different video understanding tasks and further proves that it is feasible to use datasets from various tasks for joint training. See Appendix F for complete results of GEGB.

4.3.2 Study on Data Balance Strategy for Joint Training

We should consider the varying levels of training difficulty and dataset sizes during joint training. Among all three tasks, GEGB has the largest number of training samples and the shortest trimmed video length. However, when we send all training sets from Kinetics-GEGB to our model in one epoch, the results of the other two tasks are severely affected shown in Table 2. We adopt data balance strategy during training.

This simple operation results in a significant improvement, as it can effectively balance the training for various tasks without adversely affecting GEGB’s results.

Table 3: **Study on generalization of temporal2Seq.** We compare the generalization performance from different pre-trained models on the FineAction, GTEA and TAPOS datasets. Temporal2Seq outperforms the other two for all datasets.

Model	TAD				TAS				GEGB		
	0.5	0.75	0.95	Avg	F1@{10,25,50}		Edit	Acc	0.05	Avg	
ViT-B	20.88	8.61	1.06	10.21	83.96	80.55	67.56	78.01	73.89	63.8	67.7
Baseline _{TASK}	21.14	8.74	1.10	10.37	86.71	83.22	69.23	81.68	75.53	65.2	69.5
Temporal2Seq _{data}	21.35	8.92	1.17	10.51	89.13	88.41	71.01	85.26	76.45	65.5	70.0

4.3.3 Study on the Generalization of Temporal2Seq

To further explore the effectiveness of a generalist model from joint training, we verify its transfer ability to a new dataset for each task that has not been seen. Here we treat the following three models as the pre-trained models that are fully fine-tuned on three unseen datasets for each task: **ViT-B** pre-trained on Kinetics-400, **Baseline**_[TASK] trained on one dataset for each task (THUMOS14 for TAD, Breakfast for TAS and Kinetics-GEBD for GEBD), and **Temporal2Seq**_{data} trained on all three datasets. Shown in Table 3, with the introduction of each dataset belonging to each task, the model has learned the priors from each specific dataset. So the results of **Baseline**_[TASK] are better than **ViT-B**. Furthermore, the results are further improved on all three new datasets based on **Temporal2Seq**_{data}, which demonstrates the better generalization of Temporal2Seq. See Appendix G for complete results of GEBD.

4.4 Comparison with the State-of-the-Art Methods

We compare Temporal2Seq with other task-specific methods across three tasks shown in Table 4. To ensure a fair comparison, we use ViT-B as the feature extractor for the state-of-the-art method of each task and introduce random cropping of video clips during training for the current state-of-the-art TAD method ActionFormer [59] and TAS method DiffAct [28]. From these results, we see that our method outperforms the state-of-the-art TAS method under a fair comparison, but there is still a performance gap between our Temporal2Seq with previous state-of-the-art TAD method.

Based on the above findings, we can draw two conclusions. First, the TAD detection performance of Temporal2Seq is still affected by factors like classification loss. Although weight loss simulates part of the regression capabilities, it still has a gap with mainstream regression methods and needs further improvement. Second, TAS’s existing methods demand a deeper understanding of long-term semantics. Compared with Temporal2Seq, they cannot fully utilize the semantic information within a sampling window. However, our Temporal2Seq performs worse compared with TAS methods when these methods input whole videos. Since joint training requires uniform input length, we cannot input complete videos for the TAS task since these videos are untrimmed. It is pointed out in [34] that longer temporal input will bring significant improvement in detection results. Due to space limitations, related explorations can be found in the Appendix D.

For GEBD, our Temporal2Seq is competitive with the state-of-the-art GEBD methods under fair comparison and significantly outperforms other earlier methods. We assume that it is because the GEBD dataset is a short-term trimmed video clip and random sampling can capture sufficient relevant video information. More results for GEBD are shown in Appendix F.

5 Conclusion

In this paper, we have proposed a single, unified framework of Temporal2Seq for dealing with different video understanding tasks. Temporal2Seq formulates the output of each task as a sequence of discrete tokens, which enables a unified interface via a task prompt to three tasks without consideration of designing complex heads for each task. We successfully co-train our Temporal2Seq model on three diverse video understanding tasks, covering detection, segmentation, and timestamp localization, and the experiment results empirically demonstrate the improvement of co-training across all three tasks over each individual-specific model. We also show the promising generalization ability of our trained generalist model on new datasets among these tasks.

6 Limitation

The current straightforward structure of Temporal2Seq imposes limitations on its modeling capabilities. In particular, accommodating parallel training may have side effects on tasks that depend on complete untrimmed video input, such as TAS. How to balance the temporal information requirements for different tasks needs further exploration. We hope our first attempt will inspire the following works to advance the area of generalist model design in temporal video understanding tasks.

References

- [1] Nadine Behrmann, S. Alireza Golestaneh, Zico Kolter, Jürgen Gall, and Mehdi Noroozi. Unified fully and timestamp supervised temporal action segmentation via sequence to sequence

Table 4: **Comparison with recent task-specific models on three different tasks.** For a fair comparison, we use the ViT-B as the feature extractor for the current state-of-the-art non-end-to-end methods for each task. * indicates that we input randomly cropped video clips instead of the entire video to this model in order to align with Temporal2Seq.

Method	Backbone	e2e	TAD					TAS				GEBD			
			0.3	0.4	0.5	0.6	0.7	Avg-mAP	F1@{10,25,50}	Edit	Acc	F1@0.05	Avg-F1		
Specialist Models															
RTD-Net [47]	I3D		58.5	53.1	45.1	36.4	25.0	43.6	-	-	-	-	-	-	
G-TAD [55]	TSN		66.4	60.4	51.6	37.6	22.9	47.8	-	-	-	-	-	-	
TadTR [30]	I3D		62.4	57.4	49.2	37.8	26.3	46.6	-	-	-	-	-	-	
VSGN [60]	TSN		66.7	60.4	52.4	41.0	30.4	50.2	-	-	-	-	-	-	
AFSD [25]	I3D	✓	67.3	62.4	55.5	43.7	31.1	52.0	-	-	-	-	-	-	
TALLFormer [5]	Swin-B	✓	76.0	-	63.2	-	34.5	59.2	-	-	-	-	-	-	
ActionFormer [59]	I3D		82.1	77.8	71.0	59.4	43.9	66.8	-	-	-	-	-	-	
ActionFormer* [59]	ViT-B		79.1	72.5	63.7	52.2	34.2	60.3	-	-	-	-	-	-	
MS-TCN [23]	I3D		-	-	-	-	-	-	58.2	52.9	40.8	61.4	65.1	-	
MS-TCN++ [24]	I3D		-	-	-	-	-	-	64.1	58.6	45.9	65.6	67.6	-	
UVAST [1]	I3D		-	-	-	-	-	-	76.9	71.5	58.0	77.1	69.7	-	
ASFormer [58]	I3D		-	-	-	-	-	-	76.0	70.6	57.4	75.0	73.5	-	
DiffAct [28]	I3D		-	-	-	-	-	-	80.3	75.9	64.6	78.4	76.4	-	
DiffAct* [28]	ViT-B		-	-	-	-	-	-	52.0	46.0	33.7	52.7	52.6	-	
BMN-StartEnd [26]	ResNet50		-	-	-	-	-	-	-	-	-	-	-	49.1	
TCN-TAPOS [20]	ResNet50		-	-	-	-	-	-	-	-	-	-	-	46.4	
TCN [20]	ResNet50		-	-	-	-	-	-	-	-	-	-	-	58.8	
Temporal Perceiver [48]	ResNet50		-	-	-	-	-	-	-	-	-	-	-	74.8	
Temporal Perceiver [48]	ViT-B		-	-	-	-	-	-	-	-	-	-	-	75.2	
Baseline _{TAD}	ViT-B		71.4	64.8	54.9	45.3	30.0	52.9	-	-	-	-	-	-	
Baseline _{TAS}	ViT-B		-	-	-	-	-	-	64.6	60.2	49.2	62.1	61.2	-	
Baseline _{GEBD}	ViT-B		-	-	-	-	-	-	-	-	-	-	-	71.8	
Generalist Models															
Temporal2Seq _{batch}	ViT-B		72.2	65.5	55.6	44.1	30.4	53.6	67.7	61.3	49.4	66.0	61.3	73.3	85.2
Temporal2Seq _{data}	ViT-B		71.7	64.8	55.5	44.0	31.2	53.5	66.2	60.8	50.1	64.6	62.3	73.3	85.6

translation. In *Computer Vision - ECCV 2022 - 17th European Conference, Tel Aviv, Israel, October 23-27, 2022, Proceedings, Part XXXV*, volume 13695 of *Lecture Notes in Computer Science*, pages 52–68. Springer, 2022. [3](#), [10](#), [16](#)

- [2] Tom B. Brown, Benjamin Mann, Nick Ryder, Melanie Subbiah, Jared Kaplan, Prafulla Dhariwal, Arvind Neelakantan, Pranav Shyam, Girish Sastry, Amanda Askell, Sandhini Agarwal, Ariel Herbert-Voss, Gretchen Krueger, Tom Henighan, Rewon Child, Aditya Ramesh, Daniel M. Ziegler, Jeffrey Wu, Clemens Winter, Christopher Hesse, Mark Chen, Eric Sigler, Mateusz Litwin, Scott Gray, Benjamin Chess, Jack Clark, Christopher Berner, Sam McCandlish, Alec Radford, Ilya Sutskever, and Dario Amodei. Language models are few-shot learners. 2020. [1](#), [2](#)
- [3] Hung-Shuo Chang, Chien-Yao Wang, Richard Robert Wang, Gene Chou, and Hong-Yuan Mark Liao. Yolor-based multi-task learning. *CoRR*, abs/2309.16921, 2023. [2](#), [3](#)
- [4] Ting Chen, Saurabh Saxena, Lala Li, Tsung-Yi Lin, David J. Fleet, and Geoffrey E. Hinton. A unified sequence interface for vision tasks. In *Advances in Neural Information Processing Systems 35: Annual Conference on Neural Information Processing Systems 2022, NeurIPS 2022, New Orleans, LA, USA, November 28 - December 9, 2022*, 2022. [2](#), [3](#), [5](#), [6](#)
- [5] Feng Cheng and Gedas Bertasius. Tallformer: Temporal action localization with a long-memory transformer. In *Computer Vision - ECCV 2022 - 17th European Conference, Tel Aviv, Israel, October 23-27, 2022, Proceedings, Part XXXIV*, volume 13694 of *Lecture Notes in Computer Science*, pages 503–521. Springer, 2022. [3](#), [10](#)
- [6] Michael Crawshaw. Multi-task learning with deep neural networks: A survey. *CoRR*, abs/2009.09796, 2020. [3](#)
- [7] Dima Damen, Hazel Doughty, Giovanni Maria Farinella, Antonino Furnari, Evangelos Kazakos, Jian Ma, Davide Moltisanti, Jonathan Munro, Toby Perrett, Will Price, and Michael Wray. Rescaling egocentric vision: Collection, pipeline and challenges for EPIC-KITCHENS-100. *Int. J. Comput. Vis.*, 130(1):33–55, 2022. [1](#)
- [8] Ali Diba, Mohsen Fayyaz, Vivek Sharma, Manohar Paluri, Jürgen Gall, Rainer Stiefelhagen, and Luc Van Gool. Large scale holistic video understanding. In *Computer Vision - ECCV 2020 - 16th European Conference, Glasgow, UK, August 23-28, 2020, Proceedings, Part V*, volume 12350 of *Lecture Notes in Computer Science*, pages 593–610. Springer, 2020. [2](#)

- [9] Jeff Donahue, Lisa Anne Hendricks, Sergio Guadarrama, Marcus Rohrbach, Subhashini Venugopalan, Trevor Darrell, and Kate Saenko. Long-term recurrent convolutional networks for visual recognition and description. In *IEEE Conference on Computer Vision and Pattern Recognition, CVPR 2015, Boston, MA, USA, June 7-12, 2015*, pages 2625–2634. IEEE Computer Society, 2015. 3
- [10] Long Duong, Trevor Cohn, Steven Bird, and Paul Cook. Low resource dependency parsing: Cross-lingual parameter sharing in a neural network parser. In *Proceedings of the 53rd Annual Meeting of the Association for Computational Linguistics and the 7th International Joint Conference on Natural Language Processing of the Asian Federation of Natural Language Processing, ACL 2015, July 26-31, 2015, Beijing, China, Volume 2: Short Papers*, pages 845–850. The Association for Computer Linguistics, 2015. 2, 3
- [11] Alireza Fathi, Xiaofeng Ren, and James M. Rehg. Learning to recognize objects in egocentric activities. In *The 24th IEEE Conference on Computer Vision and Pattern Recognition, CVPR 2011, Colorado Springs, CO, USA, 20-25 June 2011*, pages 3281–3288. IEEE Computer Society, 2011. 1, 7
- [12] Kristen Grauman, Andrew Westbury, Eugene Byrne, Zachary Chavis, Antonino Furnari, Rohit Girdhar, Jackson Hamburger, Hao Jiang, Miao Liu, Xingyu Liu, Miguel Martin, Tushar Nagarajan, Ilija Radosavovic, Santhosh Kumar Ramakrishnan, Fiona Ryan, Jayant Sharma, Michael Wray, Mengmeng Xu, Eric Zhongcong Xu, Chen Zhao, Siddhant Bansal, Dhruv Batra, Vincent Cartillier, Sean Crane, Tien Do, Morrie Doulaty, Akshay Erapalli, Christoph Feichtenhofer, Adriano Fragomeni, Qichen Fu, Abraham Gebreselasie, Cristina González, James Hillis, Xuhua Huang, Yifei Huang, Wenqi Jia, Weslie Khoo, Jáchym Kolár, Satwik Kottur, Anurag Kumar, Federico Landini, Chao Li, Yanghao Li, Zhenqiang Li, Karttikeya Mangalam, Raghava Modhugu, Jonathan Munro, Tullie Murrell, Takumi Nishiyasu, Will Price, Paola Ruiz Puentes, Merey Ramazanova, Leda Sari, Kiran Somasundaram, Audrey Southerland, Yusuke Sugano, Ruijie Tao, Minh Vo, Yuchen Wang, Xindi Wu, Takuma Yagi, Ziwei Zhao, Yunyi Zhu, Pablo Arbeláez, David Crandall, Dima Damen, Giovanni Maria Farinella, Christian Fuegen, Bernard Ghanem, Vamsi Krishna Ithapu, C. V. Jawahar, Hanbyul Joo, Kris Kitani, Haizhou Li, Richard A. Newcombe, Aude Oliva, Hyun Soo Park, James M. Rehg, Yoichi Sato, Jianbo Shi, Mike Zheng Shou, Antonio Torralba, Lorenzo Torresani, Mingfei Yan, and Jitendra Malik. Ego4d: Around the world in 3, 000 hours of egocentric video. In *IEEE/CVF Conference on Computer Vision and Pattern Recognition, CVPR 2022, New Orleans, LA, USA, June 18-24, 2022*, pages 18973–18990. IEEE, 2022. 1, 2
- [13] Kaiming He, Xiangyu Zhang, Shaoqing Ren, and Jian Sun. Deep residual learning for image recognition. In *2016 IEEE Conference on Computer Vision and Pattern Recognition, CVPR 2016, Las Vegas, NV, USA, June 27-30, 2016*, pages 770–778. IEEE Computer Society, 2016. 17
- [14] Y.-G. Jiang, J. Liu, A. Roshan Zamir, G. Toderici, I. Laptev, M. Shah, and R. Sukthankar. THUMOS challenge: Action recognition with a large number of classes. <http://crcv.ucf.edu/THUMOS14/>, 2014. 1, 7
- [15] Svebor Karaman, Lorenzo Seidenari, and Alberto Del Bimbo. Fast saliency based pooling of fisher encoded dense trajectories. In *ECCV THUMOS Workshop*, volume 1, page 5, 2014. 3
- [16] Enkelejda Kasneci, Kathrin Seßler, Stefan Küchemann, Maria Bannert, Daryna Dementieva, Frank Fischer, Urs Gasser, Georg Groh, Stephan Günemann, Eyke Hüllermeier, et al. Chatgpt for good? on opportunities and challenges of large language models for education. *Learning and individual differences*, 103:102274, 2023. 1, 2
- [17] Will Kay, João Carreira, Karen Simonyan, Brian Zhang, Chloe Hillier, Sudheendra Vijayanarasimhan, Fabio Viola, Tim Green, Trevor Back, Paul Natsev, Mustafa Suleyman, and Andrew Zisserman. The kinetics human action video dataset. *CoRR*, abs/1705.06950, 2017. 7, 17
- [18] Hilde Kuehne, Ali Bilgin Arslan, and Thomas Serre. The language of actions: Recovering the syntax and semantics of goal-directed human activities. In *2014 IEEE Conference on Computer Vision and Pattern Recognition, CVPR 2014, Columbus, OH, USA, June 23-28, 2014*, pages 780–787. IEEE Computer Society, 2014. 1, 7

- [19] Hilde Kuehne, Juergen Gall, and Thomas Serre. An end-to-end generative framework for video segmentation and recognition. In *2016 IEEE Winter Conference on Applications of Computer Vision, WACV 2016, Lake Placid, NY, USA, March 7-10, 2016*, pages 1–8. IEEE Computer Society, 2016. [3](#)
- [20] Colin Lea, Austin Reiter, René Vidal, and Gregory D. Hager. Segmental spatiotemporal cnns for fine-grained action segmentation. In *Computer Vision - ECCV 2016 - 14th European Conference, Amsterdam, The Netherlands, October 11-14, 2016, Proceedings, Part III*, volume 9907 of *Lecture Notes in Computer Science*, pages 36–52. Springer, 2016. [3](#), [10](#), [17](#)
- [21] Congcong Li, Xinyao Wang, Longyin Wen, Dexiang Hong, Tiejian Luo, and Libo Zhang. End-to-end compressed video representation learning for generic event boundary detection. In *IEEE/CVF Conference on Computer Vision and Pattern Recognition, CVPR 2022, New Orleans, LA, USA, June 18-24, 2022*, pages 13947–13956. IEEE, 2022. [17](#)
- [22] Hao Li, Jinguo Zhu, Xiaohu Jiang, Xizhou Zhu, Hongsheng Li, Chun Yuan, Xiaohua Wang, Yu Qiao, Xiaogang Wang, Wenhai Wang, and Jifeng Dai. Uni-perceiver v2: A generalist model for large-scale vision and vision-language tasks. In *IEEE/CVF Conference on Computer Vision and Pattern Recognition, CVPR 2023, Vancouver, BC, Canada, June 17-24, 2023*, pages 2691–2700. IEEE, 2023. [2](#), [3](#)
- [23] Shijie Li, Yazan Abu Farha, Yun Liu, Ming-Ming Cheng, and Juergen Gall. MS-TCN++: multi-stage temporal convolutional network for action segmentation. volume 45, pages 6647–6658, 2023. [3](#), [6](#), [7](#), [10](#), [16](#)
- [24] Shijie Li, Yazan Abu Farha, Yun Liu, Ming-Ming Cheng, and Juergen Gall. MS-TCN++: multi-stage temporal convolutional network for action segmentation. *IEEE Trans. Pattern Anal. Mach. Intell.*, 45(6):6647–6658, 2023. [3](#), [10](#), [16](#)
- [25] Chuming Lin, Chengming Xu, Donghao Luo, Yabiao Wang, Ying Tai, Chengjie Wang, Jilin Li, Feiyue Huang, and Yanwei Fu. Learning salient boundary feature for anchor-free temporal action localization. In *IEEE Conference on Computer Vision and Pattern Recognition, CVPR 2021, virtual, June 19-25, 2021*, pages 3320–3329. Computer Vision Foundation / IEEE, 2021. [3](#), [10](#)
- [26] Tianwei Lin, Xiao Liu, Xin Li, Errui Ding, and Shilei Wen. BMN: boundary-matching network for temporal action proposal generation. In *2019 IEEE/CVF International Conference on Computer Vision, ICCV 2019, Seoul, Korea (South), October 27 - November 2, 2019*, pages 3888–3897. IEEE, 2019. [3](#), [10](#), [17](#)
- [27] Tianwei Lin, Xu Zhao, Haisheng Su, Chongjing Wang, and Ming Yang. BSN: boundary sensitive network for temporal action proposal generation. In *Computer Vision - ECCV 2018 - 15th European Conference, Munich, Germany, September 8-14, 2018, Proceedings, Part IV*, volume 11208 of *Lecture Notes in Computer Science*, pages 3–21. Springer, 2018. [3](#)
- [28] Daochang Liu, Qiyue Li, Anh-Dung Dinh, Tingting Jiang, Mubarak Shah, and Chang Xu. Diffusion action segmentation. In *IEEE/CVF International Conference on Computer Vision, ICCV 2023, Paris, France, October 1-6, 2023*, pages 10105–10115. IEEE, 2023. [1](#), [3](#), [7](#), [9](#), [10](#), [16](#)
- [29] Qinying Liu and Zilei Wang. Progressive boundary refinement network for temporal action detection. In *The Thirty-Fourth AAAI Conference on Artificial Intelligence, AAAI 2020, The Thirty-Second Innovative Applications of Artificial Intelligence Conference, IAAI 2020, The Tenth AAAI Symposium on Educational Advances in Artificial Intelligence, EAAI 2020, New York, NY, USA, February 7-12, 2020*, pages 11612–11619. AAAI Press, 2020. [3](#)
- [30] Xiaolong Liu, Qimeng Wang, Yao Hu, Xu Tang, Shiwei Zhang, Song Bai, and Xiang Bai. End-to-end temporal action detection with transformer. *IEEE Trans. Image Process.*, 31:5427–5441, 2022. [1](#), [3](#), [10](#)
- [31] Yi Liu, Limin Wang, Yali Wang, Xiao Ma, and Yu Qiao. Fineaction: A fine-grained video dataset for temporal action localization. *IEEE Trans. Image Process.*, 31:6937–6950, 2022. [1](#), [7](#)

- [32] Ilya Loshchilov and Frank Hutter. Decoupled weight decay regularization. 2019. [7](#)
- [33] Jiasen Lu, Christopher Clark, Rowan Zellers, Roozbeh Mottaghi, and Aniruddha Kembhavi. UNIFIED-IO: A unified model for vision, language, and multi-modal tasks. 2023. [2](#), [3](#)
- [34] Emad Bahrami Rad, Gianpiero Francesca, and Juergen Gall. How much temporal long-term context is needed for action segmentation? In *IEEE/CVF International Conference on Computer Vision, ICCV 2023, Paris, France, October 1-6, 2023*, pages 10317–10327. IEEE, 2023. [9](#), [16](#)
- [35] Alec Radford, Karthik Narasimhan, Tim Salimans, Ilya Sutskever, et al. Improving language understanding by generative pre-training. 2018. [1](#)
- [36] Alec Radford, Jeffrey Wu, Rewon Child, David Luan, Dario Amodei, Ilya Sutskever, et al. Language models are unsupervised multitask learners. *OpenAI blog*, 1(8):9, 2019. [1](#)
- [37] Rajeev Ranjan, Vishal M. Patel, and Rama Chellappa. Hyperface: A deep multi-task learning framework for face detection, landmark localization, pose estimation, and gender recognition. *IEEE Trans. Pattern Anal. Mach. Intell.*, 41(1):121–135, 2019. [3](#)
- [38] Scott E. Reed, Konrad Zolna, Emilio Parisotto, Sergio Gómez Colmenarejo, Alexander Novikov, Gabriel Barth-Maron, Mai Gimenez, Yury Sulsky, Jackie Kay, Jost Tobias Springenberg, Tom Eccles, Jake Bruce, Ali Razavi, Ashley Edwards, Nicolas Heess, Yutian Chen, Raia Hadsell, Oriol Vinyals, Mahyar Bordbar, and Nando de Freitas. A generalist agent. *Trans. Mach. Learn. Res.*, 2022, 2022. [3](#)
- [39] Marcus Rohrbach, Sikandar Amin, Mykhaylo Andriluka, and Bernt Schiele. A database for fine grained activity detection of cooking activities. In *2012 IEEE Conference on Computer Vision and Pattern Recognition, Providence, RI, USA, June 16-21, 2012*, pages 1194–1201. IEEE Computer Society, 2012. [3](#)
- [40] Sebastian Ruder. An overview of multi-task learning in deep neural networks. *CoRR*, abs/1706.05098, 2017. [3](#)
- [41] Dian Shao, Yue Zhao, Bo Dai, and Dahua Lin. Intra- and inter-action understanding via temporal action parsing. In *2020 IEEE/CVF Conference on Computer Vision and Pattern Recognition, CVPR 2020, Seattle, WA, USA, June 13-19, 2020*, pages 727–736. Computer Vision Foundation / IEEE, 2020. [7](#), [17](#)
- [42] Dingfeng Shi, Yujie Zhong, Qiong Cao, Jing Zhang, Lin Ma, Jia Li, and Dacheng Tao. React: Temporal action detection with relational queries. In *Computer Vision - ECCV 2022 - 17th European Conference, Tel Aviv, Israel, October 23-27, 2022, Proceedings, Part X*, volume 13670 of *Lecture Notes in Computer Science*, pages 105–121. Springer, 2022. [1](#), [3](#)
- [43] Mike Zheng Shou, Stan Weixian Lei, Weiyao Wang, Deepti Ghadiyaram, and Matt Feiszli. Generic event boundary detection: A benchmark for event segmentation. In *2021 IEEE/CVF International Conference on Computer Vision, ICCV 2021, Montreal, QC, Canada, October 10-17, 2021*, pages 8055–8064. IEEE, 2021. [1](#), [7](#)
- [44] Mike Zheng Shou, Stan Weixian Lei, Weiyao Wang, Deepti Ghadiyaram, and Matt Feiszli. Generic event boundary detection: A benchmark for event segmentation. In *2021 IEEE/CVF International Conference on Computer Vision, ICCV 2021, Montreal, QC, Canada, October 10-17, 2021*, pages 8055–8064. IEEE, 2021. [3](#), [17](#)
- [45] Sebastian Stein and Stephen J. McKenna. Combining embedded accelerometers with computer vision for recognizing food preparation activities. In *The 2013 ACM International Joint Conference on Pervasive and Ubiquitous Computing, UbiComp '13, Zurich, Switzerland, September 8-12, 2013*, pages 729–738. ACM, 2013. [1](#)
- [46] Haisheng Su, Weihao Gan, Wei Wu, Yu Qiao, and Junjie Yan. BSN++: complementary boundary regressor with scale-balanced relation modeling for temporal action proposal generation. In *Thirty-Fifth AAAI Conference on Artificial Intelligence, AAAI 2021, Thirty-Third Conference on Innovative Applications of Artificial Intelligence, IAAI 2021, The Eleventh Symposium on Educational Advances in Artificial Intelligence, EAAI 2021, Virtual Event, February 2-9, 2021*, pages 2602–2610. AAAI Press, 2021. [3](#)

- [47] Jing Tan, Jiaqi Tang, Limin Wang, and Gangshan Wu. Relaxed transformer decoders for direct action proposal generation. In *2021 IEEE/CVF International Conference on Computer Vision, ICCV 2021, Montreal, QC, Canada, October 10-17, 2021*, pages 13506–13515. IEEE, 2021. [3](#), [10](#)
- [48] Jing Tan, Yuhong Wang, Gangshan Wu, and Limin Wang. Temporal perceiver: A general architecture for arbitrary boundary detection. *IEEE Trans. Pattern Anal. Mach. Intell.*, 45(10):12506–12520, 2023. [1](#), [3](#), [8](#), [10](#), [17](#)
- [49] Jiaqi Tang, Zhaoyang Liu, Chen Qian, Wayne Wu, and Limin Wang. Progressive attention on multi-level dense difference maps for generic event boundary detection. In *IEEE/CVF Conference on Computer Vision and Pattern Recognition, CVPR 2022, New Orleans, LA, USA, June 18-24, 2022*, pages 3345–3354. IEEE, 2022. [1](#), [3](#), [5](#), [17](#)
- [50] Kevin D. Tang, Li Fei-Fei, and Daphne Koller. Learning latent temporal structure for complex event detection. In *2012 IEEE Conference on Computer Vision and Pattern Recognition, Providence, RI, USA, June 16-21, 2012*, pages 1250–1257. IEEE Computer Society, 2012. [3](#)
- [51] Ashish Vaswani, Noam Shazeer, Niki Parmar, Jakob Uszkoreit, Llion Jones, Aidan N. Gomez, Lukasz Kaiser, and Illia Polosukhin. Attention is all you need. pages 5998–6008, 2017. [3](#), [4](#)
- [52] Chenhao Wang, Hongxiang Cai, Yuxin Zou, and Yichao Xiong. RGB stream is enough for temporal action detection. *CoRR*, abs/2107.04362, 2021. [3](#)
- [53] Limin Wang, Bingkun Huang, Zhiyu Zhao, Zhan Tong, Yinan He, Yi Wang, Yali Wang, and Yu Qiao. Videomae V2: scaling video masked autoencoders with dual masking. In *IEEE/CVF Conference on Computer Vision and Pattern Recognition, CVPR 2023, Vancouver, BC, Canada, June 17-24, 2023*, pages 14549–14560. IEEE, 2023. [4](#), [7](#)
- [54] Saining Xie, Ross B. Girshick, Piotr Dollár, Zhuowen Tu, and Kaiming He. Aggregated residual transformations for deep neural networks. In *2017 IEEE Conference on Computer Vision and Pattern Recognition, CVPR 2017, Honolulu, HI, USA, July 21-26, 2017*, pages 5987–5995. IEEE Computer Society, 2017. [2](#), [3](#)
- [55] Mengmeng Xu, Chen Zhao, David S. Rojas, Ali K. Thabet, and Bernard Ghanem. G-TAD: sub-graph localization for temporal action detection. In *2020 IEEE/CVF Conference on Computer Vision and Pattern Recognition, CVPR 2020, Seattle, WA, USA, June 13-19, 2020*, pages 10153–10162. Computer Vision Foundation / IEEE, 2020. [3](#), [10](#)
- [56] Min Yang, Guo Chen, Yin-Dong Zheng, Tong Lu, and Limin Wang. BasicTAD: An astounding rgb-only baseline for temporal action detection. *Comput. Vis. Image Underst.*, 232:103692, 2023. [3](#)
- [57] Serena Yeung, Olga Russakovsky, Ning Jin, Mykhaylo Andriluka, Greg Mori, and Li Fei-Fei. Every moment counts: Dense detailed labeling of actions in complex videos. *Int. J. Comput. Vis.*, 126(2-4):375–389, 2018. [3](#)
- [58] Fangqiu Yi, Hongyu Wen, and Tingting Jiang. Asformer: Transformer for action segmentation. *arXiv preprint arXiv:2110.08568*, 2021. [1](#), [3](#), [5](#), [6](#), [7](#), [10](#), [16](#)
- [59] Chen-Lin Zhang, Jianxin Wu, and Yin Li. Actionformer: Localizing moments of actions with transformers. In *Computer Vision - ECCV 2022 - 17th European Conference, Tel Aviv, Israel, October 23-27, 2022, Proceedings, Part IV*, volume 13664 of *Lecture Notes in Computer Science*, pages 492–510. Springer, 2022. [1](#), [3](#), [9](#), [10](#)
- [60] Chen Zhao, Ali K. Thabet, and Bernard Ghanem. Video self-stitching graph network for temporal action localization. In *2021 IEEE/CVF International Conference on Computer Vision, ICCV 2021, Montreal, QC, Canada, October 10-17, 2021*, pages 13638–13647. IEEE, 2021. [3](#), [10](#)
- [61] Xizhou Zhu, Jinguo Zhu, Hao Li, Xiaoshi Wu, Hongsheng Li, Xiaohua Wang, and Jifeng Dai. Uni-perceiver: Pre-training unified architecture for generic perception for zero-shot and few-shot tasks. In *IEEE/CVF Conference on Computer Vision and Pattern Recognition, CVPR 2022, New Orleans, LA, USA, June 18-24, 2022*, pages 16783–16794. IEEE, 2022. [3](#)

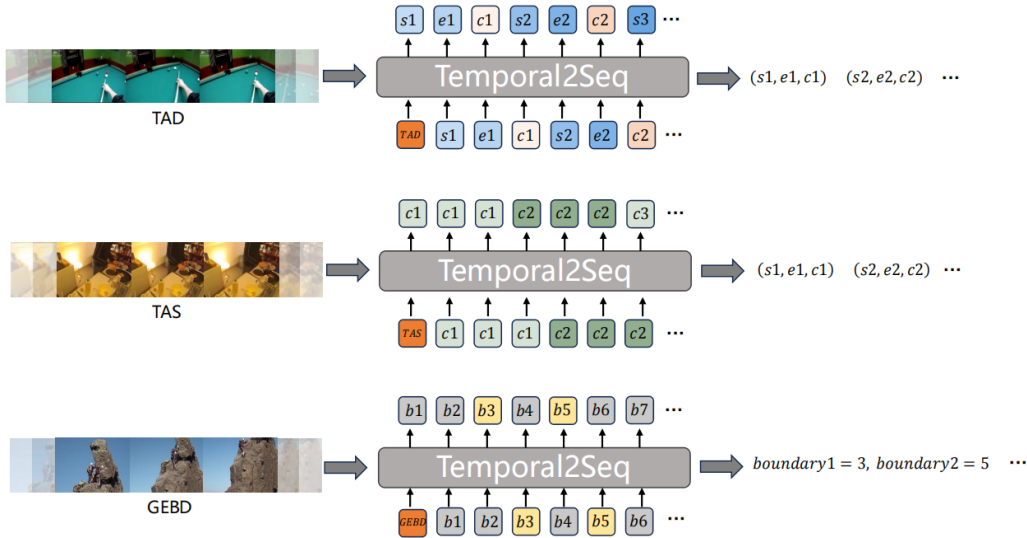


Figure 5: **More details of inference.** Here we visualize the Temporal2Seq inference process for three tasks.

Appendix / supplemental material

A More Details of Data Balance Strategy

As shown in Table 2 in the main text, Applying joint training directly will have side effects on the TAD and TAS tasks. To solve such a problem, we make the following attempt, that is, instead of completely training the entire GEBD dataset in each epoch, we complete one epoch training after completing training for TAS and TAD datasets, which means only part of the randomly sampled data is trained within an epoch for GEBD datasets. We first try this manner on **Temporal2Seq_{batch}** and stop training when the batches of TAS and TAD datasets are fully trained in one epoch. We then apply this idea to **Temporal2Seq_{data}** and align it with batch-mixing configuration by directly sampling GEBD data before training.

B More Details of Inference

As shown in Figure 5, we describe how the prediction results are obtained during inference. For each task, we use a sliding window to sample video clips during inference and input them into the model for inference. Given each prompt token $[TASK]$, Temporal2Seq outputs the predictions auto-regressively. Each task has its own token space. After that, these predicted tokens will be transformed into predictions for each task.

For TAD, we start with $[TAD]$ as the start token and give triplet predictions based on input video clips. We found that the prediction results are not given in the order of actions, that is, there is no sequential relationship between the two predicted consecutive actions (s_i, e_i, c_i) and $(s_{i+1}, e_{i+1}, c_{i+1})$. This shows that temporal2seq did not learn the sequential relationship between TAD actions. This also shows that in the existing TAD dataset, the correlation between actions is not high, leading to redundancy in action prediction. So we need non-maximum suppression to remove redundant predictions.

For TAS, we start with $[TAS]$ as the start token and give frame-by-frame action category predictions. They are then converted into dense segment-level segmentation results in the form of triplets, where $e_i = s_{i+1} - 1$.

For GEBD, we start with $[GEBD]$ as the start token and output each frame’s binary predictions. The token position predicted as a boundary will be converted into an action boundary. Specifically,

Table 5: **Effectiveness of Weight Loss.** Here we build the baseline and report mAP with all tIoU thresholds for TAD.

Dataset	Model	Loss	0.3	0.4	0.5	0.6	0.7	Avg
THUMOS14	Baseline _{TAD}	cross entropy	70.3	63.8	54.4	43.4	29.2	52.2
		weight loss	71.4	64.8	54.9	45.3	30.0	52.9

Table 6: **Comparison Between Results for Different Window Size.** Here we build the baseline for TAS. The longer the sampling window, the better the prediction results.

Dataset	Model	Window Size(sec.)	F1@{10,25,50}			Edit	Acc
Breakfast	Baseline _{TAS}	40	64.6	60.2	49.2	62.1	61.2
		80	67.1	61.7	51.5	65.6	62.0
		160	69.0	63.6	51.6	68.8	65.0
		320	77.1	72.2	56.6	75.7	68.1
	MS-TCN [23]	Full Video	58.2	52.9	40.8	61.4	65.1
	MS-TCN++ [24]	Full Video	64.1	58.6	45.9	65.6	67.6
	UVASt [1]	Full Video	76.9	71.5	58.0	77.1	69.7

we give the location prediction of the boundary based on its relative position within the temporal sampled window.

C Effectiveness of Weight Loss for TAD

We compare our **weight loss** with cross-entropy loss based on **Baseline_{TAD}** trained from THUMOS14, an individual task model for TAD. Shown in Table 5. The use of weight loss has resulted in improved accuracy in detection results (from 52.2 to 52.9). This suggests that using simple classification loss to supervise detection tasks is not the optimal choice. Although such a sequence-to-sequence autoregressive framework can transform all perception tasks into a classification task in token space, it is necessary to recognize the distinctions between classification and regression tasks and design different supervision schemes.

D Effectiveness of Long-term Context for TAS

When building **Baseline_{TAS}** for TAS trained from Breakfast, we randomly crop a clip from the video and send it to our Temporal2Seq framework for training instead of training the entire video to accommodate parallel training with other tasks. As shown in Table 6, we find a performance gap between our method and the traditional TAS methods [58; 23; 28]. Inspired by [34], we conduct ablations with different input window sizes on Breakfast and obtain a similar conclusion, indicating that a longer context is advantageous for TAS compared to shorter ones.

However, a longer window size means more frames must be input, while Kinetics-GEBD only contains 300 frames. During joint training, an input of 300 frames can only guarantee a window size of 40 seconds for the Breakfast. We are forced to make a compromise here and randomly crop a clip of 40 seconds with $\tau = 4$ from the video for TAS and stack these clips into batches in subsequent co-training experiments.

E Study on Different Prediction Paradigms for TAD

Table 7: **Study on prediction paradigm for TAD.** Here we apply dense prediction paradigm for TAD and the detection results are bad.

task	paradigm	0.3	0.4	0.5	0.6	0.7	Avg
TAD	sparse	71.4	64.8	54.9	45.3	30.0	52.9
	dense	47.9	42.7	34.9	25.1	16.0	33.3

Our Temporal2Seq designs a sparse detection paradigm for the TAD task in the main text, where we give consecutive triples represented as (s_i, e_i, c_i) as detection results. Here we attempt to apply

the dense prediction paradigm adopted by both TAS and GEBD tasks for TAD to unify the training paradigm of all three tasks. However, as shown in Table 7, the detection results are worse than the sparse paradigm by a large margin, indicating that the dense paradigm is unsuitable for temporal action detection.

F Full Results of Comparison With Recent Task-specific Models on GEBD

Table 8: **Comparison with the event-level state-of-the-art methods in terms of f1@Rel.Dis on Kinetics-GEBD validation set.** Previous work uses ResNet50 [13] as the feature extractor. For a fair comparison, we use the ViT-B as the feature extractor for the current state-of-the-art non-end-to-end method Temporal Perceiver.

Model	Backbone	f1@Rel.Dis.										
		0.05	0.1	0.15	0.2	0.25	0.3	0.35	0.4	0.45	0.5	Avg
Specialist Models												
BMN [26]	ResNet50	18.6	20.4	21.3	22.0	22.6	23.0	23.3	23.7	23.9	24.1	22.3
BMN-StartEnd [44]	ResNet50	49.1	58.9	62.7	64.8	66.0	66.8	67.4	67.8	68.1	68.3	64.0
TCN-TAPOS [44]	ResNet50	46.4	56.0	60.2	62.8	64.5	65.9	66.9	67.6	68.2	68.7	62.7
TCN [20]	ResNet50	58.8	65.7	67.9	69.1	69.8	70.3	70.6	70.8	71.0	71.2	68.5
PC [44]	ResNet50	62.5	75.8	80.4	82.9	84.4	85.3	85.9	86.4	86.7	87.0	81.7
Temporal Perceiver [48]	ResNet50	74.8	82.8	85.2	86.6	87.4	87.9	88.3	88.7	89.0	89.2	86.0
Temporal Perceiver [48]	CSN	82.2	88.0	89.9	90.9	91.6	92.0	92.3	92.5	92.7	92.9	90.5
Temporal Perceiver [48]	ViT-B	75.2	82.5	84.8	86.2	87.0	87.5	88.0	88.3	88.6	88.9	85.7
E2E [21]	ResNet50	74.3	83.0	85.7	87.2	88.0	88.6	89.0	89.3	89.6	89.8	86.5
DDM-Net [49]	ResNet50	76.4	84.3	86.6	88.0	88.7	89.2	89.5	89.8	90.0	90.2	87.3
Baseline _{GEBD}	ViT-B	71.8	79.7	83.0	85.1	86.5	87.5	88.2	88.7	89.1	89.5	84.9
Generalist Models												
Temporal2Seq _{batch}	ViT-B	73.3	80.7	83.8	85.5	86.7	87.6	88.0	88.6	89.0	89.2	85.2
Temporal2Seq _{data}	ViT-B	73.3	80.9	84.0	85.9	87.1	88.0	88.6	89.0	89.3	89.6	85.6

Due to space limitations in the text, here we give the results under all relative thresholds of Kinetics-GEBD shown in Table 8. It can be seen that Temporal2Seq under the two training strategies can achieve good results at each threshold compared with these task-specific methods.

Table 9: **Study on Generalization of Temporal2Seq on TAPOS [41].** We compare the generalization performance from different pre-trained models on TAPOS datasets. Temporal2Seq outperforms the other two for all datasets on each threshold.

Model	f1@Rel.Dis.										
	0.05	0.1	0.15	0.2	0.25	0.3	0.35	0.4	0.45	0.5	Avg
ViT-B	63.8	66.3	67.2	67.9	68.3	68.6	68.7	68.8	68.9	69.0	67.7
Baseline _{task}	65.2	68.0	69.1	69.8	70.0	70.4	70.5	70.6	70.7	70.8	69.5
Temporal2Seq _{data}	65.5	68.7	69.6	70.3	70.6	70.9	71.1	71.2	71.3	71.4	70.0

G Full results on Generalization of Temporal2Seq on GEBD

Due to space limitations in the text, here we give the results under all relative thresholds of TAPOS shown in Table 9. We compare three pre-trained models: ViT-B pre-trained on Kinetics-400 [17], the pre-trained specific model Baseline_{task} on one dataset for each task (Kinetics-GEBD for GEBD), and our pre-trained generalist model Temporal2Seq trained on three tasks. It can be seen that Temporal2Seq can achieve good results at each threshold compared with the other two.

H Broader Impacts

In this paper, we used public datasets and related evaluation metrics to explore the feasibility of joint training on the temporal video understanding task. Our Temporal2Seq enables a unified interface via a task prompt to three tasks without consideration of designing complex heads for each task and shows the promising generalization ability on new datasets among these tasks. This successful attempt will lead to subsequent work for further in-depth exploration and even address the limitations of this work.